01 (45)-AF:Modelo-AF 8/20/11 6:23 AM Page 87

A Cellular Automata Based Multi-Process Microfabrication Simulator

Fábio B. Colombo[1], Marcelo N. P. Carreño[2]

[1,2]Fábio B. Colombo and Marcelo N. P. Carreño, Electronic Systems Engineering Department,
Universidade de São Paulo, São Paulo, Brazil
e-mail: fabio.colombo@usp.br

ABSTRACT

We describe a 3D simulator for several fabrication techniques utilized to create MEMS. The software is based on a cellular automata model and allows the user to simulate several processes, such as anisotropic wet etching in alkaline solutions and deep reactive-ion etching (DRIE) on (100) oriented Si substrates. The simulator allows for arbitrarily shaped masking materials and several processes can be applied in sequence to the same substrate. This enables the software to simulate the fabrication of complex MEMS devices which require more than one etching step. So, we show examples of fabrication processes involving different combinations of substrate wet and plasma DRI etching. Although relatively simple automata were utilized for the simulations, the results are in excellent accordance with reported experimental results. At this moment the simulations do not consider physical parameters affecting the fabrication process, the results shown here are important from an engineering point of view for qualitative analyses. At this moment more sophisticated automata are in development to simulate other processes, like film deposition (with different degrees of anisotropy) on previously etched substrates.

Index Terms: cellular automata, simulation, microfabrication.

INTRODUCTION

The anisotropic wet etching of silicon in alkaline solutions is still a fundamental microfabrication technique in the development and fabrication of microeletromechanical systems (MEMS). Wet anisotropic etching permits one to manufacture, at a low cost, thin membranes, cantilevers and other self-sustained structures that have different degrees of freedom to perform mechanical movement. These movements are a key factor in many MEMS-based sensors and actuators. This technique can also be used to fabricate static microstructures or microsystems that are useful due to their 3D topology, like Si microtips and Si microchannels for microfluidic systems. One thing both types of microstructures have in common is the complex 3D geometry involved in the fabrication process. This geometry is related to the Si crystallographic planes and varies during the etching process. The 3D shape of the microstructure depends on the etching time (and other parameters, such as etchant and temperature) in such a complex way that it quickly becomes difficult to predict. This is one of the primary motivations to develop an anisotropic etching simulator.

Several types of simulators for Si wet etching have been reported in the literature. Some are based on geometric considerations, such as the Wulff-Jaccodine method [1] and its variations, such as Eshapes [2]. However atomistic simulators based either on Kinetic Monte Carlo (KMC) or Cellular Automata (CA) have shown good results and wide applicability [3][4], leading to more precise simulations and allowing deeper analysis. With this concern, we have previously reported on a CA based anisotropic Si wet etch simulator [4].

With the growth in usage and development of MEMS, several other techniques have been developed to create structures that cannot be fabricated using only traditional wet anisotropic etching or to allow for compatibility with microelectronics in the same wafer. Processes that use several techniques, not only wet etching, allow for the fabrication of more complex microstructures, and to be able to simulate the entire process is highly desirable.

Motivated by this, we now present a multi-process CA based simulator which, along with the already reported anisotropic wet etch simulations, is also able to simulate other processes like deep reactive-ion etching (DRIE) and film etching and deposition, all in sequence and on the same substrate.

01 (45)-AF:Modelo-AF 8/20/11 6:23 AM Page 88

SI SUBSTRATE INITIATION

We use a simple cellular automaton with a few optimizations to simulate wet etching. The automaton is a Basic Cellular Automata (BCA) [5] and will be described later. It is important to note, however, that the reason the BCA works is strongly linked to the geometry of crystalline Si. Therefore, correctly describing the Si lattice of the substrate is important.

This is a relatively simple task if we desire to create substrates with a single orientation. In our case, this orientation is (100). Although we are able to create a crystal by simply repeating the Si diamond unit cell, as pictured in Figure 1, this has the drawback of instantiating boundary atoms twice by the superposition of neighboring cells. This is illustrated in Figure 1b, where the superposed atoms are marked in a lighter color. In order to correctly simulate etching one of these atoms will need to be removed later.

However, there exists a simpler basic cell that does not instantiate atoms at the boundaries twice. This simplified cell, pictured in Figure 1c below, can be created by removing the atoms that will be repeated if two unit cells are placed side by side. Since it is possible to run a CA in a regular lattice, we are able to run the etching CAs directly on the Si structure shown in Figure 1.

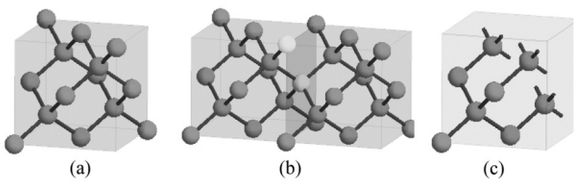

Figure 1. A silicon diamond unit cell is pictured in (a). Two neighboring cells with superposed atoms, in a lighter color, are pictured in (b). A simplified cell that allows for repetition without superposition is pictured in (c).

This structure, however, is not ideal to simulate the deposition of films over the Si substrate using CA. A three dimensional matrix of cubic cells is better suited for this task. It is possible to store a Si lattice in a cubic matrix. There are several ways to do this. The simplest is to simply store the atoms in exactly the way they are laid out in our simplified cell. Each simplified cell occupies a volume of 4x4x4 matrix spaces that will contain eight atoms. All other spaces will be empty. This is not ideal for two reasons: a) we must waste memory storing empty spaces between atoms; and b) film deposition is complicated since we must not deposit film in the empty spaces between the atoms.

A condensed three-dimensional matrix similar to the one described in [3] was used to solve this problem. In this case only the eight atoms that make up the simplified cell are stored. Therefore each simplified cell occupies a volume of only 2x2x2 matrix spaces. Atoms are slightly translated in this setup, which is not ideal, however we can render atoms in the correct position when visualizing the results, which minimizes this problem.

ANISOTROPIC WET ETCH SIMULATOR

A cellular automaton consists of a regular grid of cells of a finite number of dimensions. The grid may or may not be finite. Initially each cell is in one of several finite states. At each step, the state of each cell is updated according to a set of rules, which take into consideration a certain neighborhood. The neighborhood is a group of cells usually defined around the cell and may or may not include the cell itself.

All cells have their state updated at exactly the same instant. Our cell grid is the Si lattice built following the rules described earlier, each atom being considered a CA cell. As shown in previous works [3][5], the neighborhood to be considered when updating the state of an atom includes all atoms directly linked to it, the so called first neighbors, and all atoms directly linked to the first neighbors, the so called second neighbors.

Since the simulator deals with intrinsic undoped semiconductors, the cells can be in one of three states: Atom, Empty and Mask. A cell in the Atom state represents an atom in the Si substrate that has not been removed. A cell in the Empty state represents an atom that has been removed. A cell in the Mask state represents the masking material being used in the etching process. The simulation itself is based on the transition rules stated below:

1. If a cell is in the Atom state and has less than 3 first neighbors, its state is changed to Empty;
2. If a cell is in the Atom state and has 3 first neighbors and less than 9 second neighbors, its state is changed to Empty;
3. If a cell is in the Atom state with any other configuration, then its state is not changed;
4. If a cell is in the Mask or Empty state, its state is not changed.

The rules described above are based on the anisotropy observed when Si is etched in alkaline solutions of KOH. Rule 1 defines how {100} planes will be etched since atoms in this plane have two complete bonds and two incomplete bonds (see Figure 2a). Rule 2 will etch {110} planes but not {111} planes. Although atoms on both planes have the same number of first neighbors, {110} atoms are bonded to atoms on the plane surface while all bonds for atoms on any {111} plane are with atoms in the bulk (see Figure 2b and Figure 2c).

As we can see by the transition rules the automaton is deterministic. The transition rules are based solely on the neighborhoods of the atoms. This has the advantage of producing results that are more uniform than an automaton that uses a removal probability function. However in our case, as opposed to automata that use removal probability functions, etch rates are defined purely by the geometry of the Si lattice.

01 (45)-AF:Modelo-AF 8/20/11 6:23 AM Page 89

Etch time may be defined by fitting the automaton (001) etch rate to the desired values. In order to do this we must define two values: the distance between two consecutive layers of the (001) plane and the duration of a time step. When we say the distance must be fitted, we mean that a value different from the actual value for a Si diamond unit cell can be used. For example, if we define the distance to be 1 μm and the time step to be 0.02 hour, then the etch rate for (001) Si plane will be 50 μm/h [6]. The other etch rates will be automatically fitted due to the geometry.

As an example, take the etch rate of the (110) plane. As per our rules, at each step a full layer of atoms is removed from both (001) and (110) planes. But the distance between (110) layers is equal to $\sqrt{2}$ times the distance between (001) planes. Therefore the etch rate for {110} planes will always be $\sqrt{2}$ times larger than that for {100} planes. Using the same values as before, the etch rate for the (110) plane would be approximately 70.7 μm/h.

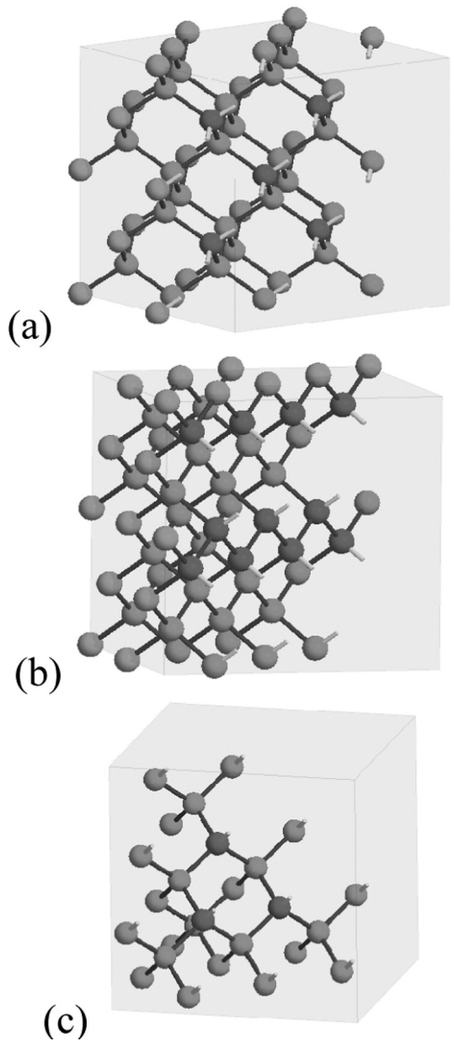

Figure 2. Atomic configurations in plane families {100} (a), {110} (b) and {111} (c). Atoms on the plane surface are rendered in a darker color and missing bonds have half the length of normal bonds.

DRIE SIMULATOR

A simple simulator for DRIE processes was also added. The simulator takes as input a substrate and a masking material. It runs on the same lattice described before. As a rule we remove all cells on the surface in the Atom state not directly under the masking material. This simulates the expected behavior for a DRIE. However it does not take into account other effects, such as reductions in etch rate at higher depths or the loading effect.

In a similar fashion to the BCA, it is necessary to define only the distance between two consecutive (001) planes, since only (100) Si wafers are available, and the duration of a time step. Defining these values will define the etch rate.

FILM ETCHING AND DEPOSITION SIMULATOR

The simulator also allows the user to deposit and selectively etch a film that will be used as masking material for the substrate etching processes. It is able to deposit the film representing the masking material on top of the previously described Si lattice. The film deposition simulator is based on a simple cellular automata that uses an expanded Moore neighborhood. This neighborhood includes all 27 cells in the 3x3x3 cube where the central cell is the cell being analyzed. The automaton can be simply described: if a cell is in an Empty state and any of its neighbors are not in an empty state, the cell changes to the Mask state, otherwise its state remains unchanged.

The film etching is done selectively using a “photolithographic mask“. The user inputs an image, or two in case of a double sided etching, where red pixels are used to determine which areas of the masking material are to be protected. All cells in the Mask state below a red pixel, i.e. with the same x and y coordinates, are considered protected. The bottom mask works in a similar manner; all cells above a red pixel are protected.

The etching automaton uses a simpler neighborhood consisting of two cells: the one above and the one below the cell being analyzed. The rules are also not complex:

1. If a cell is in the Mask state and the top neighbor is empty and the top mask does not protect the cell, the cell changes its state to Empty.
2. A cell will also change its state to Empty if it is in the Mask state, the neighbor cell below the cell is in the Empty state and the bottom mask does not protect the cell.
3. In any other conditions the cell state remains unchanged.

The user is not required to enter a bottom mask when performing a single sided etching operation.

01 (45)-AF:Modelo-AF 8/20/11 6:23 AM Page 90

RESULTS

The software

Substrates of any size can be used. The limiting factor is the memory usage to store the lattice. Lattices with up to 6 million atoms can be simulated with a normal desktop computer. Simulation times depend on the size of the exposed surface. This is due to the fact that only the states of cells on the surface are update at each step. Visualization uses OpenGL and a graphics card will increase performance. The software has been run and tested on OS X, Windows XP, Windows Vista and Windows 7 operating systems.

The BCA

The BCA is a simple automaton, but it is able to generate satisfactory results in many situations. For example, consider Figure 3 where we show the results for simulation using only the BCA to describe the formation of a Si microtip. The software renders all currently exposed atoms. Colors are used to indicate neighbor count. Blue atoms have three first neighbors, green atoms have two first neighbors and yellow atoms have a single first neighbor and atoms with no neighbors are rendered in red. Only atoms on the surface are rendered. This serves two purposes. First it lowers the amount of processing necessary to render results. It also allows better visualization of the results since atoms in the bulk do not obstruct the users' view. The masking material, which is made up of the cells in the Mask state, is rendered as a translucent red layer.

The simulations show a lot of similarity to an actual microtip fabricated using KOH wet etching, especially the top, which has a characteristic eight-sided shape. The base is not so similar, as it reaches higher up than expected. Also the base has a square shape and there is no inflection which is also observed on real microtip, as can be seen in Figure 3. At 94 steps the base of the (111) triangles pictured in Figure 3 both have approximately 10 μm. Assuming the spacing between layers of the (001) plane to be 0.5 μm so as to have the cross arms with a width of 50μm, the resulting microtip will have a height of 64 μm. This is slightly larger than the experimental results of 52 μm [7].

The time to etch all the Si under the arms is around 20 minutes. Since this stage takes 53 steps in the simulator, each step lasts approximately 22.6 seconds. The final etch time to fabricate the tip seen in Figure 3, which is disconnected from the masking material, is therefore close to 49 minutes. This is close to measured experimental values [8]. Both the experimental and simulation images in Figure 3 use masking material with the same geometry.

Multi-process Simulations

As was mentioned before, we can also simulate more than one etching process. As an example, consider

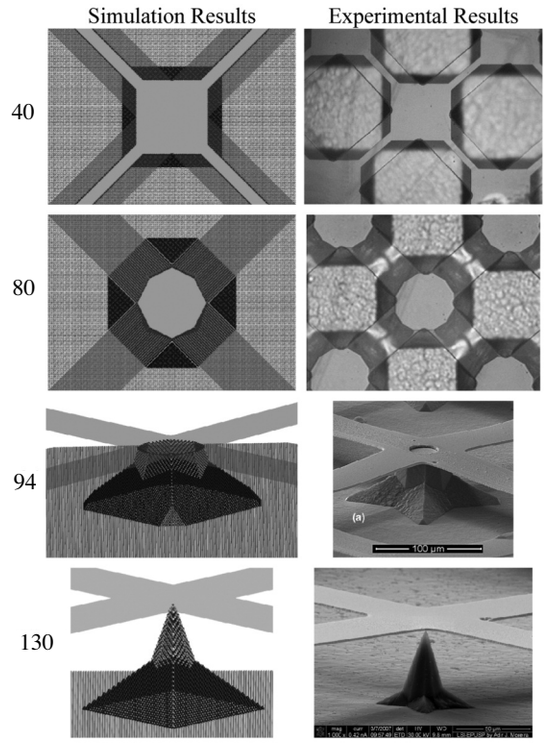

Figure 3. Wet etching steps to make a microtip. Top and side views are shown for real and simulated results. The numbers near the images indicate number of steps simulated. The slightly darker material, forming and X, is the masking material used for the simulation.

the results shown in Figure 4. It shows a simulation where a Si substrate is wet etched using a masking material with a square opening until a {111} pyramidal cavity is formed. Wet etching is paused, the masking material is removed and wet etching is then resumed. A similar process can be used, for example, in the fabrication of aspherical optics [9].

The results shown in Figure 4 are a side view of the substrate being etched. The substrate is located below the masking material. Once again, it is not rendered so as to not obstruct the view of the pyramidal cavities that will be formed. The software is able, however, to render the bulk in case the user wishes to see it. We have added to the captured image a gray area below the mask to show the volume occupied by the bulk in the initial configuration.

The simulation results are similar to the expected. First we observe the typical formation of the inverted pyramidal cavity with the {111} walls and, after removing the masking material, the formation of a new cavity. This is a wider, shallower pyramidal cavity, since its walls make an angle of 25.2º (see Figure 5) with the wafer surface, which is also etched. We also observe that, in opposition of what occurs with the pyramid with {111} walls, this new pyramid continues its growth after reaching the apex. In fact, we observe, in accordance with the experimental results, the formation of a new plane at the bottom that grows as etching continues.

01 (45)-AF:Modelo-AF 8/20/11 6:23 AM Page 91

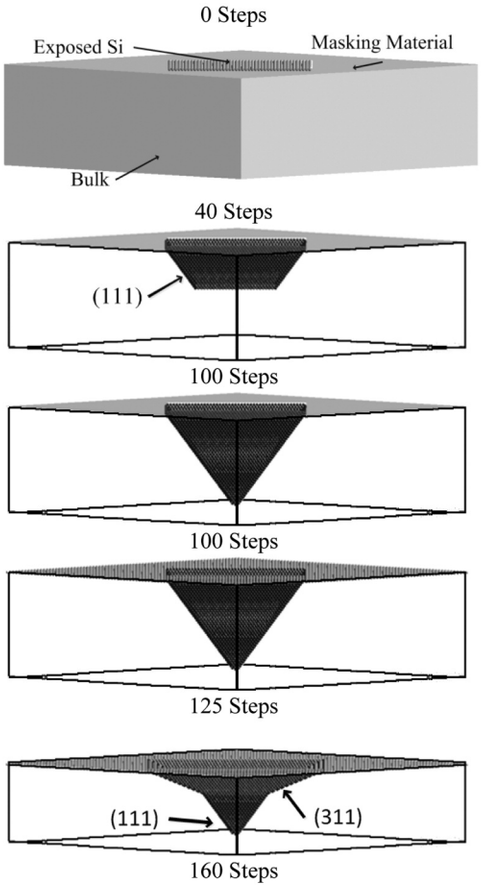

Figure 4. From steps 0 to 100, etching is carried out with the masking material. From steps 100 to 160, etching is carried out without the masking material. In the detail, the direction in which the bottom plane grows. The results show only the surface of the Si substrate; atoms inside the bulk are not rendered. The pyramidal cavities are seen from the side through the bulk of the Si substrate. A representation of the bulk was added to all images. The last image shows the direction of growth of the new emergent (100) plane.

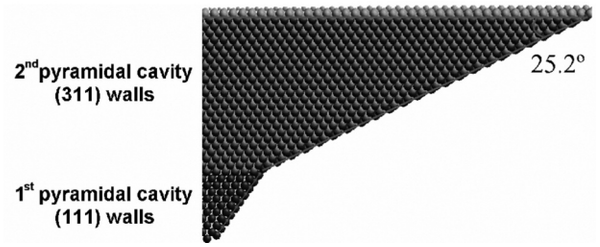

Figure 5. Angle between the substrate surface and the walls of the second pyramidal cavity, formed when the masking material is removed and wet etching is resumed. This image is similar to Figure 4 after 125 steps. This angle indicates that these planes belong to the {311} family and not the expected {411} as reported by the literature [9].

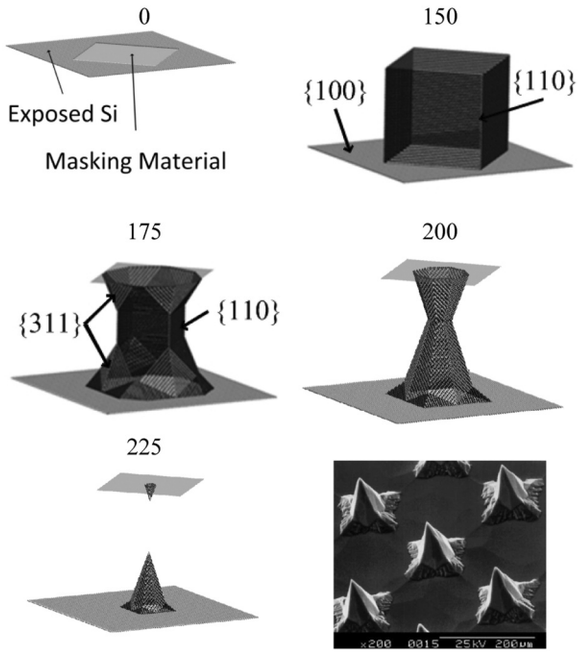

Figure 6. Time evolution of a microtip fabrication using DRIE to create a column and wet etching techniques to transform the column into a microtip. The values near the images indicate the number of steps to arrive at that state. In the last image we have the experimental results from [10]. The experimental results have a similar shape to the experimental results.

However, we do not observe any rounding effect as observed in experimental results. In fact, one of the major uses of this type of process is to obtain a semi spherical etching profile utilizing a non-expensive and easy to implement anisotropic wet etching process in KOH solutions. In order to simulate this effect, new phenomenon must be included in the corrosion model. Furthermore, the planes that emerge from our simulation when the masking material is removed (the second pyramidal walls) belong to the {311} family and not the expected {411} reported by the literature [9].

The simulator is capable of simulating other processes along with wet etching. A typical simulation result is shown in Figure 6, where we also simulate the process to fabricate a Si microtip, but unlike the previous example, here we carried out DRIE etch followed by an anisotropic wet etch. As we can see, first we use the DRIE simulator module to create a large column and after that, without removing the masking material, we utilized the BCA module to simulate anisotropic wet etching on the resulting column.

As we can see from Figure 6, a microtip is created similar to the one in [10]. Instead of mechanical dicing, we simulated a DRIE dicing. Note that this dicing exposes the {110} planes that initial form the sides of the column. When we begin wet etching, the planes that appear are very similar to the expected experimental results. After 175 steps, we can see the {111} planes that form near the base and near the top of the column, underneath the masking material. Also visible, marked by the alternating blue-green atoms, are the {311} planes that will etch away the {111} planes and later form the final microtip.

01 (45)-AF:Modelo-AF 8/20/11 6:23 AM Page 92

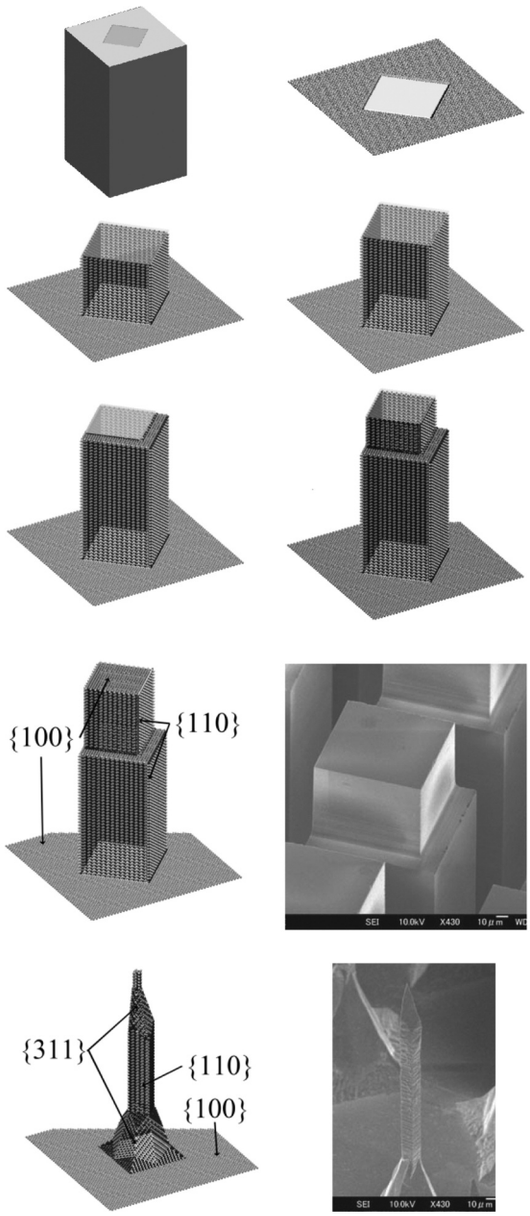

Figure 7. Etching a Si microtip using DRIE and wet etching techniques. The first image shows the bulk. Next we see a sequence to create the columns. In the lower right corner we have an image from [11] of the initial structure the authors use and the microtip produced after wet etching.

Since the simulator allows for the deposition and selective etching of the masking material, we are also able to simulate processes that require not a simple removal but a change in the shape of the masking material. To demonstrate we will simulate the fabrication of a microtip by another method. As with the previous microtip, we use a square shaped masking material to generate a Si column. We then etch the masking material once again so that it will cover only part of the top of this initial column. The simulator allows this second etch to be done directly, but it is also possible to remove the masking material completely, deposit a new layer covering the entire etched substrate, and selectively etch this new masking material.

We then resume DRIE to create small indentations on the top of the column. These indentations will provide a sharp tip to the column. The next step involves completely removing the remaining masking material. After this removal, we start wet etching the substrate to form the microtips. The images below show these various steps. For simplicity we simply etched the masking material a second time to generate the second masking material shape used to create the indentations. The results obtained in the simulator, pictured in Figure 7, are similar to the results in [11]. Once again DRIE was used to simulate the mechanical dicing process used by the authors in [11].

CONCLUSIONS

The results shown here prove that the software is able to simulate the microfabrication processes of several types of devices. As a work in progress, it still has some limitations. It was built as an improvement over previous software [4] and was designed to allow multiple types of etching to be carried out as a means to broaden the scope of its application. We feel that the software achieves this goal and currently provides a base framework that can be expanded to simulate other microfabrication processes, such as isotropic etching and multiple film depositions.

The software can be improved in several ways. As shown in Figure 4, the aspherical lens fabrication simulation did not show results similar to the expected experimental results. In fact, there are no parameters that can be adjusted in the BCA to change this. We previously showed how to calculate the etch rate for the (110) plane when the etch rate for the (001) plane is known. The ratio between these two rates is always fixed and this is true for all crystallographic planes. Etch rates, and therefore plane selectivity, are mostly determined by the Si geometry and are fixed. They do not vary with KOH concentration or temperature since these variables are not considered during simulation. The fact that BCA presents results similar to the experimental results is probably due to the fact that wet etching in KOH is also strongly dependent on the geometry of Si.

Therefore an automaton that allows for better etch rate fitting, such as the continuous cellular automata described in [5] and [3] will be implemented. This type of automaton provides smooth results like the BCA but is capable of better etch rate fitting, which in turns produces better simulation results for {n11} plane etching.

The DRIE simulation is very simplistic in the fact that it always generates straight downward walls. However, the results described here are the first step for more realistic models that can fit the several morphological effects observed in real etch experiment utilizing the different available plasma based techniques.

01 (45)-AF:Modelo-AF 8/20/11 6:23 AM Page 93

We are currently developing other functionalities for the multi-process simulator, to allow for a broader range of MEMS microfabrication processes to be simulated using the software. In particular, development of modules for film deposition capable of simulating CVD and PVD with different degrees of anisotropy and growth conformity are currently underway. We are also working on an isotropic etching module. All these expansions will be described in future works.

ACKNOWLEDGEMENTS

The authors would like to acknowledge FAPESP (Process Nº 2009/06766-0) and CNPq (Nº 306292/2004-1) for their financial support.

REFERENCES

1. R. J. Jaccodine, "Use of modified free energy theorems to predict equilibrium growing and etching shapes", *Journal of Applied Physics*. Vol. 33, 1962, p. 2643.
2. T. J. Hubbard, and E. K. Antonsson, "Emergent faces in crystal etching", *Journal of Microeletromechanical Systems*, Vol. 3, Mar 1994, p. 19.
3. J. P. de Oliveira Jr., "Desenvolvimento de um software para simulação atomística de corrosão anisotrópica do silício por autômato celular", Master Thesis, Department of Electronic Systems Engineering, Polytechnic School of the University of São Paulo, São Paulo, 2008.
4. J.P. de Oliveira Jr. and M.N.P. Carreño, "Simulation of anisotropic etching of silicon using a Cellular Automata model", *ECS Transactions : Microelectronics Technology and Devices - SBMicro 2008*, Vol.14, Nº 1, 2008, p. 37-46.
5. M. A. Gosálvez et al., "Atomistic methods for the simulation of evolving surfaces", *Journal of Micromechanics and Microengineering*, Vol. 18, April, 2008.
6. H. Seidel et al., "Anisotropic Etching of Crystalline Silicon in Alkaline Solutions", *Journal of the Eletrochemichal Society*, Vol. 137, 1990, p. 3612-3626.
7. M. Z. Mielli et al., "Fabrication of Silicon Microtips with Integrated Electrodes", *Journal Integrated Circuits and Systems,* Vol. 3, 2008, p. 97-103.
8. A. L. Barros. *Desenvolvimento de Micropontas de Silício com Eletrodos Integrados para Dispositivos de Emissão por Efeito de Campo*. Master Thesis, Department of Electronic Systems Engineering, Polytechnic School of the University of São Paulo, São Paulo, 2007.
9. D. W. de Lima Monteiro et al., "Single-mask microfabrication of aspherical optics using KOH anisotropic etching of Si", *OPTICS EXPRESS*, Vol. 11, No. 18, September, 2003, p. 2244-2252.
10. M. Shikida et al., " Non-photolithographic pattern transfer for fabricating arrayed three-dimensional microstructures by chemical anisotropic etching", *Sensors and Actuators A*., Vol. 116, June, 2004, p. 264-271.
11. M. Shikida et al., "Non-photolithographic pattern transfer for fabricating pen-shaped micro needle structures", *J. Micromech. Microeng*. Vol. 14, No.11, 2004, p. 1462–1467.